Supplemental Materials

Use of face information varies systematically from developmental prosopagnosics to super-recognizers

Tardif, J., Morin Duchesne, X., Cohan, S., Royer, J., Blais, C., Fiset, D., Duchaine, B., & Gosselin, F.

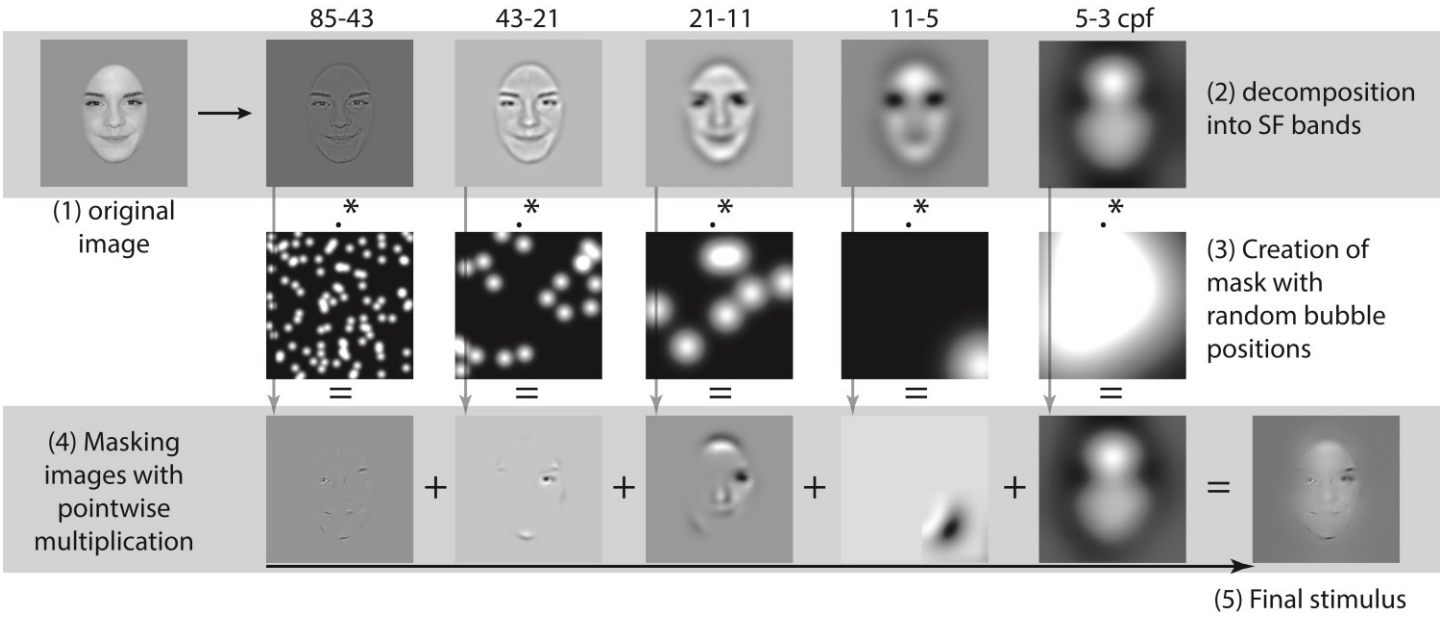

Figure S1 – Step-by-step method for the creation of spatially randomly sampled stimuli on each trial. (1) In the original image, external features are masked using a single ellipse, and images are aligned with each other on the main features of the face. (2) The image is decomposed into six spatial-frequency bands. For clarity, the sixth band is not depicted here. It is used as a background for all stimuli. (3) The spatial location of the Gaussian windows (bubbles) is randomly selected. A Gaussian window of different size is applied to each spatial-frequency band so that the same number of cycles is revealed by one bubble. (4) Separately for each spatial-frequency band, the random mask is multiplied pointwise with the filtered image. (5) The final stimulus is created by adding together all 5 randomly sampled filtered images (along with the 6^{th}, lowest spatial-frequency filtered image). The final stimulus therefore consists of visual information randomly sampled through space and spatial-frequency.

	PCA first component (CFMT and CFPT)	PCA first component (all four indices)	CFMT	CFPT	Number of bubbles
PCA 1st component (four indices)	0.937**				
CFMT	0.899**	0.882**			
CFPT	-0.908**	-0.812**	-0.632**		
№ bubbles	-0.538**	-0.706**	-0.507**	0.465**	
№ faces identified	0.557**	0.734**	0.595**	0.416**	-0.301*

Table S1 – Pearson correlation coefficients between each of the ability scores tested (N=112; **p<.01; *p<.05 Bonferroni-corrected for 10 tests). The global ability index, used in the article, is the first component obtained by running a PCA on the CFMT and CFPT scores. We also computed the first component of a PCA ran on all four ability measures (see Figure S4).

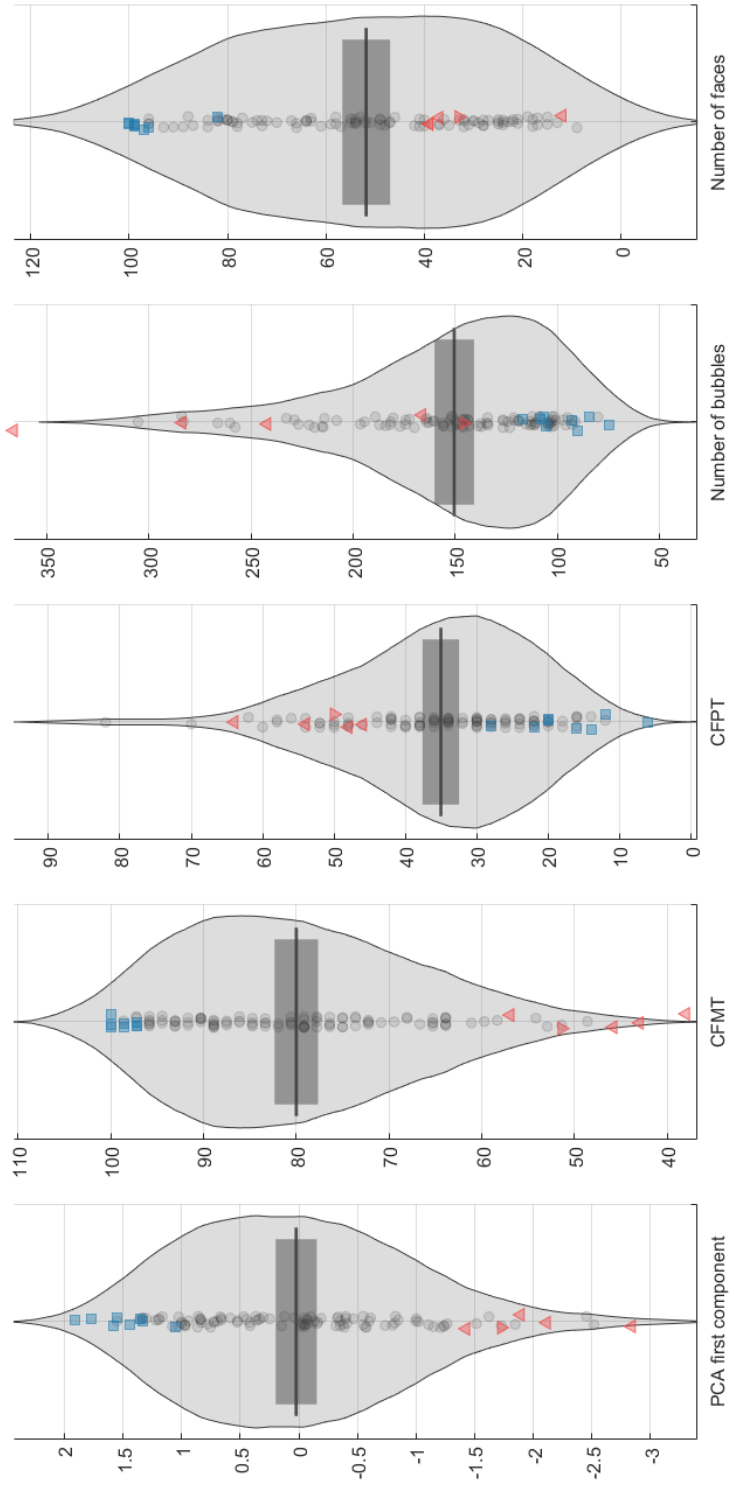

Figure S2 – Pirate plots representing individual differences in face-recognition abilities in our sample (N=112). Triangles represent Developmental Prosopagnosics (DPs) and squares, Super-recognizers (SRs). The inverted triangle represents the DP recruited from the general population. Pirate plots were developed by Nathaniel D. Phillips (Phillips, N.D., 2017. YaRrr! The Pirate's Guide to R. APS Observer, 30(3); we used a Matlab adaptation freely available and coded by Adelino P. Silva; https://github.com/adelinocpp/Pirate-Plot-Matlab).

	Developmental prosopagnosics						Super-recognizers								
	DP1*	DP2	DP3	DP4	DP5	$\bar{x}$ (*sd*)	SR1	SR2	SR3	SR4	SR5	SR6	SR7	SR8	$\bar{x}$(*sd*)
CFMT	51.4	45.8	38.0	56.9	43.0	47.0 (*7.4*)	100	97.2	98.6	97.2	97.2	100	100	98.6	98.6 (1.3)
CFPT	50	54	64	48	46	52.4 (7.1)	20	20	28	6	14	12	22	16	17.3 (6.8)
N° faces	33	12	37	39	39	32 (11.4)	100	97	99	99	99	96	82	100	96.5 (6.0)
N° Bub.	146.0	242.1	366.0	166.4	283.6	240.8 (89.5)	105.9	108.5	107.0	74.7	84.7	117.3	90.2	93.3	97.7 (14.3)

Table S2 – Raw data of each SR and DP subject on each face-recognition ability measure. Subject numbers match those of the individual classification images in Figure S5. Note that all these participants were recruited as DPs and SRs based on their face-recognition performances in prior studies (SRs: Cohan, Nakamaya & Duchaine, 2016; DPs: Guo, Yang & Duchaine, 2016; Guo et al., 2017), except DP1* who was identified as a DP only after data analysis.

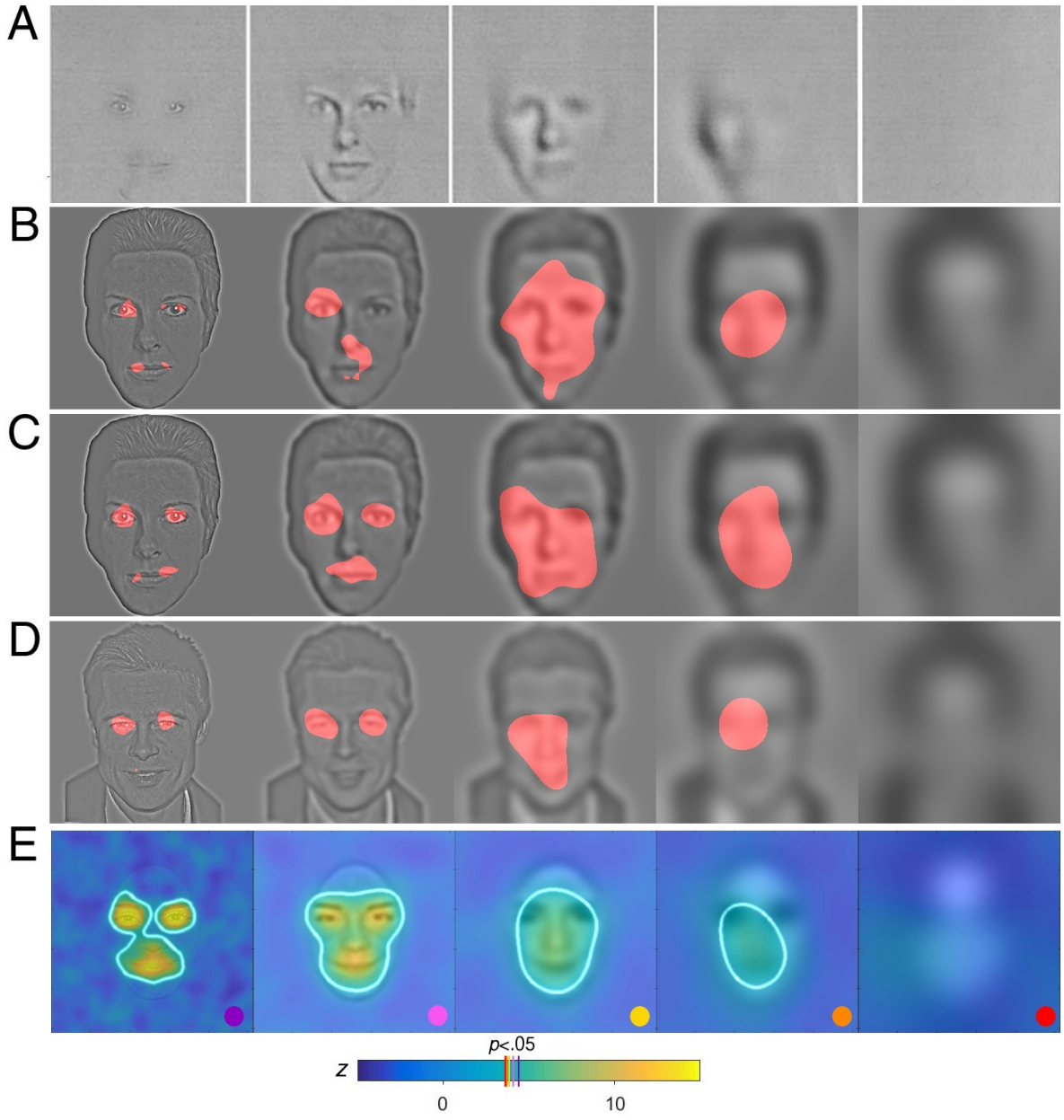

Figure S3 – Classification images showing the average use of information for face identification in (A) Gosselin and Schyns (2001; 20 participants each completed 500 trials, for a total of 10,000 trials), (B) Schyns, Bonnar and Gosselin (2002; 15 participants each completed 500 trials, for a total of 7,500 trials), (C) Caldara et al. (2005; 7 participants each completed 4,200 trials, for a total of 29,400 trials), (D) Butler et al. (2010; 40 participants completed an average of 180 trials, for a total of 7,212 trials), and (E) in the present study (112 subjects completed a total of 111,885). Significant facial areas ($p<.05$) are either shown in (A), coloured in red in (B), (C) and (D), or delimited by a solid white line in (E). Note that the larger number of trials in our study results in a larger signal-to-noise ratio, leading to higher z-scores, and more significant pixels.

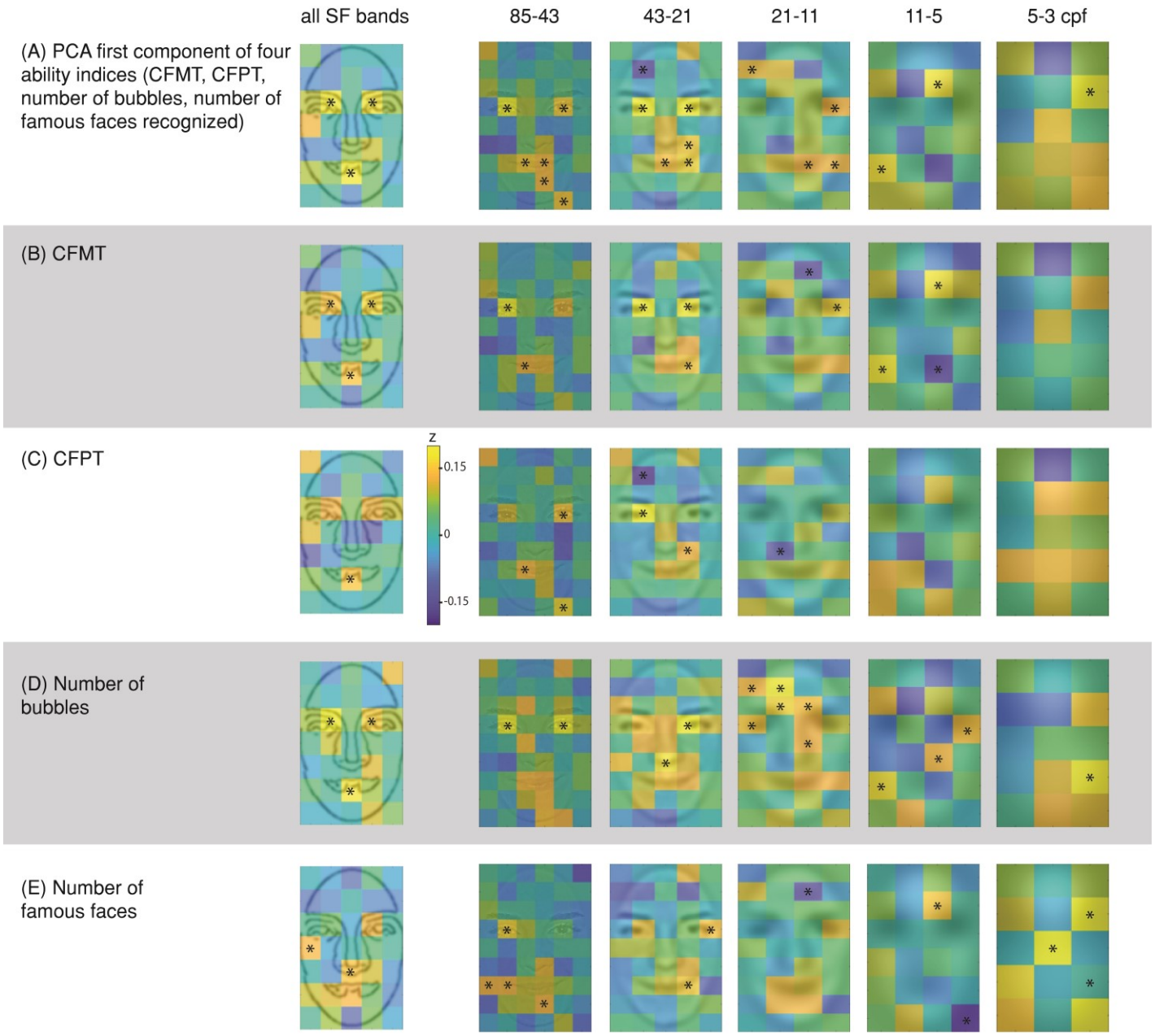

Figure S4 – Robustness of the relationship between use of information and face-recognition ability. In (A), regularized multiple linear regressions were performed on the use of information and the first component of a PCA ran on all four face-recognition ability indices. This first PCA component explained 61.7% of the variance, loaded positively on the four indices, and had an eigenvalue of 2.55 while the other components' eigenvalues were below 1. The model collapsed over SFs (leftmost image) explained 49% (adjusted R^2=0.494; k=45.35) of the variance of this PCA first component. In (B), regularized multiple linear regressions were performed on the use of information and the raw CFMT scores (adjusted R^2 = 0.43; k=55.80 for the model collapsed over SFs). In (C), regularized multiple linear regressions were performed on the use of information and the raw CFPT scores (adjusted R^2 = 0.308; k=41.65 for the model collapsed over SFs). In (D), regularized multiple linear regressions were performed on the use of information and minus the number of bubbles required to maintain an accuracy of 75% correct (adjusted R^2 = 0.519; k=40.15 for the model collapsed over SFs). In (D), regularized multiple linear regressions were performed on the use of information and the number of faces recognized (adjusted R^2 = 0.343; k=42.70 for the model collapsed over SFs). Significant rectangles are identified with asterisks ($p<.05$; permutation test with 5000 iterations). Note the similarities between the models as well as the ones presented in the body of the article.

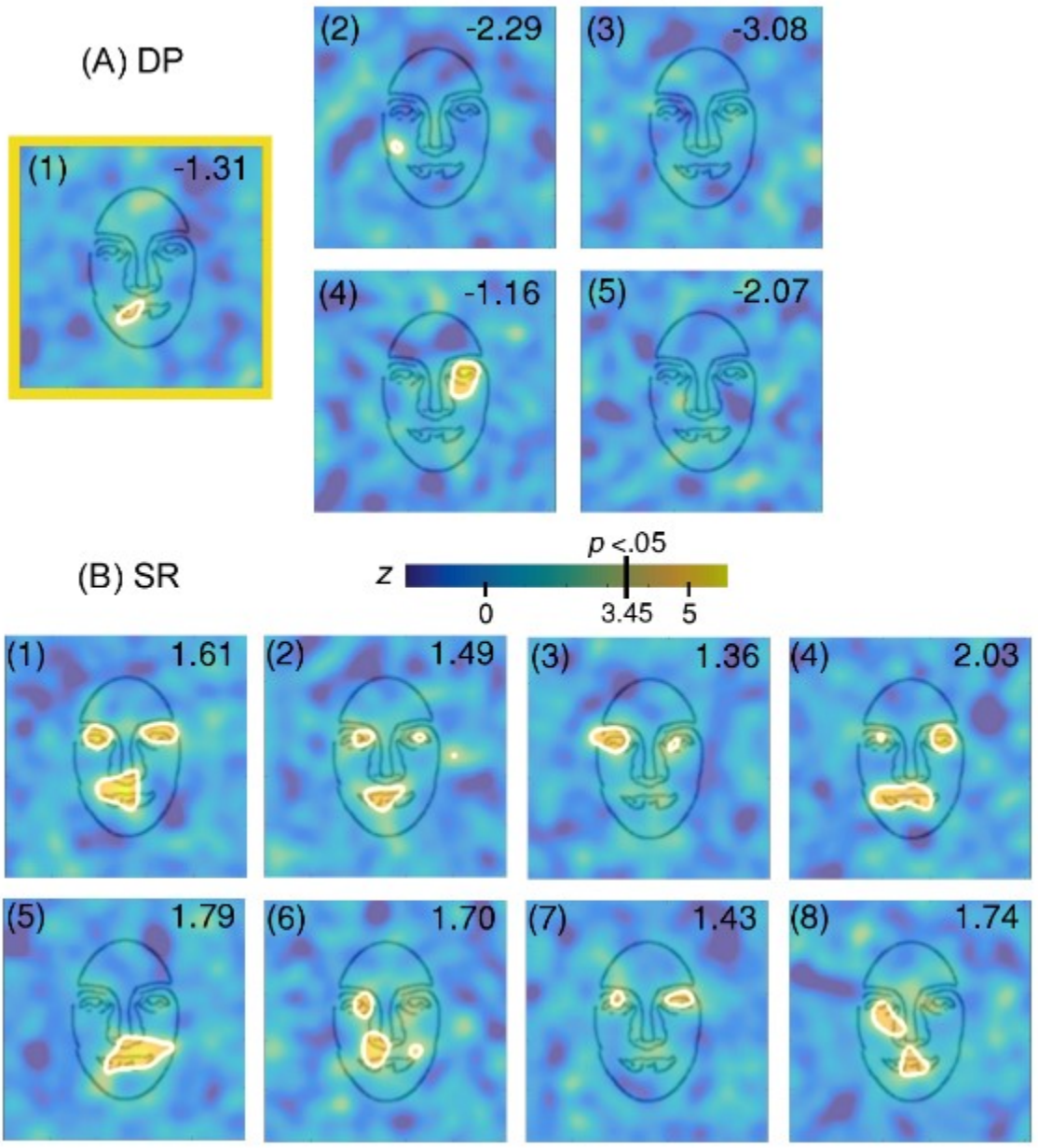

Figure S5 – Individual classification images of (A) the five developmental prosopagnosics and (B) the eight super-recognizers. White lines delineate the facial information that is used above statistical threshold ($p<.05$; threshold $z=2.9$; $\sigma=10$; $S_r=15{,}204$). Global individual ability z-scores are shown in the top right corner of each CI (see Table S2 for details). Note that all these participants were recruited as DPs and SRs based on their face-recognition performances in prior studies, except DP1* who was identified as a DP only after data analysis.

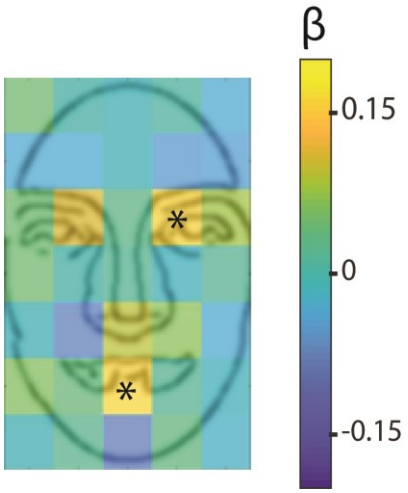

Figure S6 – Results of second-order regularized multiple linear regressions on participants with intermediate face-recognition abilities (N=99; excludes SRs and DPs), where the colour of each element represents its regression coefficients (*p<.05, determined using a 5000-iteration permutation test), or the level at which the particular area predicts the global index of performance (first component of the PCA conducted on CFMT and CFPT scores). When SF bands are collapsed, the model explains 41.9% of the variance (k=44.35), and 65% of the variance in abilities for SR and DP participants.